

# Formation of diffusion nitride-oxide coatings

*Urol Boynazarov\**

Karshi Engineering-Economics Institute, Karsh, Uzbekistan

**Abstract.** It is known that nitro-oxide coatings were developed based on nitriding, which are obtained using a two-stage technology consisting of nitriding at the first stage of the process and vaporization at the second stage. Such processing provides high physical and mathematical characteristics of hardened parts.

This technological process was improved by us due to preliminary oxidation, which made it possible to accelerate the production of nitride-oxide with the necessary physical and mechanical properties.

This work makes a theoretical calculation of the oxidation processes and subsequent nitriding of steels and a comparison with experimental data on the example of 38X2MYA. The article presents an analysis of the formation of oxynitride diffusion protective layers obtained by a three-stage nitriding method at a temperature of 580° C, which consists of preliminary oxidation, nitriding, and subsequent steam oxidation. The article also describes the effect of the oxide film on the nitriding process during preliminary oxidation and nitriding under short-term conditions at a temperature of 580 S.

## 1 Introduction

The medium of chemical-thermal treatment by nitriding is one of the promising methods of surface hardening, which allows some physical and mechanical properties of parts operating in the loading mode, particularly friction and corrosion. However, obtaining such a protective diffusion coating by the existing nitriding process, such as nitriding and subsequent vapor oxidation, requires more time and a lot of energy costs. Nitriding with preliminary and subsequent vapor oxidation in optimal modes can significantly reduce the production time with good diffusion protective coatings properties and save energy [1-3].  
MRT

## 2 Methods

To study the kinetics of the formation of diffusion layers during nitriding in ammonia with preliminary and subsequent oxidation in water vapor, samples of commercial iron and structural steels were used: 38Kh2MYuA, 40Kh (GOST 1050-74, GOST 4543-71).

---

\*Corresponding author: [boynazarov\\_63@mail.ru](mailto:boynazarov_63@mail.ru)

**Table 1.** The chemical composition of studied steels

Steel grade	Content of elements, % (by weight)					
	<i>C</i>	<i>Si</i>	<i>Mn</i>	<i>Cr</i>	<i>Al</i>	<i>Mo</i>
38X2MYuA	0.39	0.29	0.3	1.4	1.0	0.2
40X	0.41	0.29	0.55	0.96	-	-

Before chemical-thermal treatment, the surface of the samples was ground, polished, and degreased in acetone; the surface roughness was = 0.10 – 0.20  $\mu\text{m}$ .

An example of the result of calculating the pre-oxidation process at an oxidation temperature of 580 °S and an oxidation time of 10 minutes is shown in Fig 1.a. After oxidation, an oxide layer with a thickness of about 5  $\mu\text{m}$  is formed on the surface.

The greatest difficulty is describing the nitriding process of a sample that has undergone preliminary oxidation. In this case, nitriding and deoxidation of the surface layer occur simultaneously. The diffusion coefficients of nitrogen at a given depth depend on the oxygen concentration at the same distance from the surface [11].

The equations describing nitrogen diffusion take the following form:

$$\frac{dC_{\alpha}(x,t)}{dt} = D_{\alpha}(x) \frac{d^2C_{\alpha}(x,t)}{dx^2} \quad (1)$$

$$\frac{dC_{\gamma'}(x,t)}{dt} = D_{\gamma'}(x) \frac{d^2C_{\gamma'}(x,t)}{dx^2} \quad (2)$$

$$\frac{dC_{\varepsilon}(x,t)}{dt} = D_{\varepsilon}(x) \frac{d^2C_{\varepsilon}(x,t)}{dx^2} \quad (3)$$

Where  $C_{\alpha}(x,t), C_{\gamma'}(x,t), C_{\varepsilon}(x,t)$  are nitrogen concentration in  $\alpha$ -,  $\gamma'$ - and  $\varepsilon$ -phases  
 $D_{\alpha}(x), D_{\gamma'}(x), D_{\varepsilon}(x)$  are the diffusion coefficients of nitrogen in the  $\alpha$ -,  $\gamma'$ - and  $\varepsilon$ -phases;  $t$ -time.

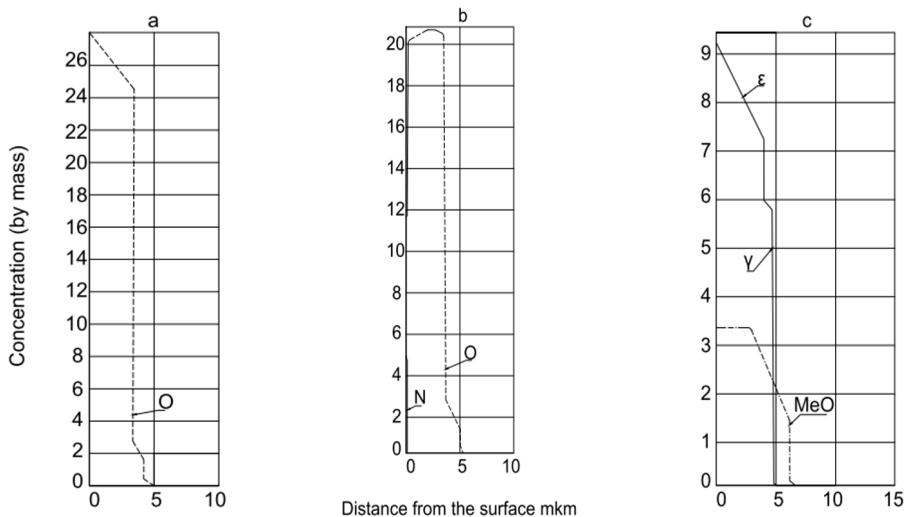


**Fig. 1.** Influence of oxide film on nitriding process. Operating modes: *a* is preliminary oxidation at a temperature of 580°C, for 10 minutes; *b* is preliminary oxidation at a temperature of 580 °C, for 10 minutes + nitriding at 580 °C, for 5 minutes; *c* is preliminary oxidation at a temperature of 580°C for 10 minutes + nitriding at 580 °C for 15 minutes.

The diffusion coefficients depend on the x coordinate since the oxygen concentration changes with the coordinate, and in fact, they depend on the oxygen concentration at this depth x.

Mass balance equations at the boundaries of phase transitions:

$$(C_{\epsilon\gamma'} - C_{\gamma'\epsilon}) \frac{d\xi_{\epsilon\gamma'}}{dt} = [D_{\gamma'}(x) \frac{dC_{\gamma'}(x,t)}{dx} - D(x) \frac{dC_{\epsilon}(x,t)}{dx}]_{x=\xi_{\epsilon\gamma'}(t)} \quad (4)$$

$$(C_{\gamma'\epsilon} - C_{\alpha\gamma'}) \frac{d\xi_{\alpha\gamma'}}{dt} = [D_{\alpha}(x) \frac{dC_{\alpha}(x,t)}{dx} - D_{\gamma'}(x) \frac{dC_{\gamma'}(x,t)}{dx}]_{x=\xi_{\alpha\gamma'}(t)} \quad (5)$$

Where  $C_{\alpha\gamma'}$ ,  $C_{\gamma'\omega}$ ,  $C_{\epsilon\gamma'}$ ,  $C_{\gamma'\epsilon}$ , are equilibrium concentrations at the interfaces;

$\xi_{\alpha\gamma'}(t)$ ,  $\xi_{\epsilon\gamma'}(t)$  are the coordinates of the phase boundaries. Similar equations are drawn up to describe the oxygen diffusion process, while the oxygen diffusion coefficients also depend on the nitrogen concentration at a given point.

The diffusion equations for nitrogen and oxygen, considering the presence of phase transitions, were solved numerically by the finite difference method. In this case, the method of through counting was used, which was proposed in [4] to solve the Stefan problem in the theory of heat conduction. Since concentration (as opposed to temperature) is a discontinuous function, the unknown functions in the diffusion equations were transformed into continuous ones. After finding new functions, the reverse transformation was performed [1, 11].

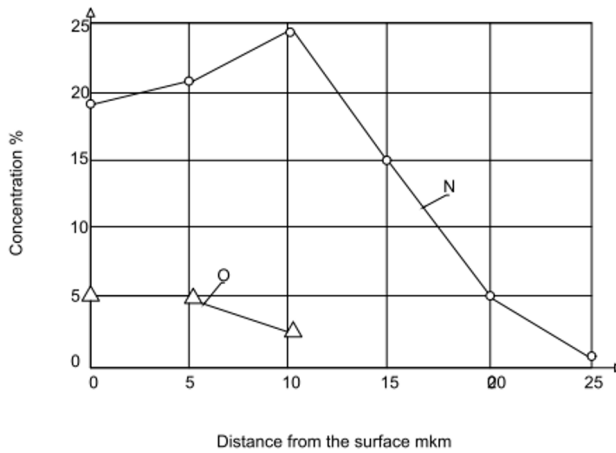


**Fig. 2.** Distribution of oxygen and nitrogen after preliminary oxidation:580°C; 10 min. + nitriding 580°C; 2 hours.

At the beginning of the nitriding process, oxygen leaves the sample's surface; however, the thickness of the resulting  $\epsilon$  and  $\gamma'$ - phases is small (Fig. 1.b shows the calculated curve 5 minutes after the start of nitriding).

The oxide film remaining behind a thin layer of  $\epsilon$ - and  $\gamma'$ -phases prevents the growth of the nitride layer. Subsequently, the oxide film becomes thinner and disappears; the nitride layer grows rapidly (Fig. 1.). In the area where the oxide film used to be, the internal oxidation of *Ma*, *Cr*, and probably *Al* occurs.

The presence of oxides in the region of the former oxide zone is confirmed by the results of Auger spectroscopy. Fig. 2 shows the distributions of oxygen and nitrogen concentrations obtained by Auger spectroscopic analysis. At a depth of about 5 microns, oxygen is present in an amount not exceeding 5%. The oxygen concentration in the oxide film (for example,  $Fe_3O_4$ ) is much higher. The concentration of oxygen dissolved in the

matrix is much lower. The Auger analysis results are explained by the formation of oxides of alloying elements in place of the former oxide film [5, 6, 7].

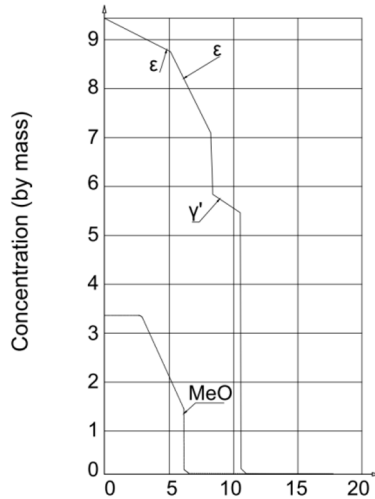


**Fig. 3.** Distribution of oxygen and nitrogen concentrations after nitriding: treatment mode: preliminary oxidation: 580oC; 10 min. + nitriding 580oC; 30 min.

Since the alloying elements form oxides in the region of the former oxide film, they impede the diffusion of nitrogen in the  $\epsilon$  phase to a lesser extent, and the diffusion coefficient of nitrogen in the  $\epsilon$ -phase (where the oxide film used to be) increases. In fig. 3 shows the calculated distribution of nitrogen and oxygen concentrations after 30 minutes of nitriding. A break occurs on the distribution curve of the nitrogen concentration in the  $\epsilon$ -phase region at a distance of 6  $\mu\text{m}$  from the surface (which, as can be seen from the oxygen distribution, corresponds to the former boundary of the oxide film). This break is explained by different diffusion coefficients in the  $\epsilon$  - phase on different sides of the break point [1, 2, 3].

An increase in the diffusion coefficient of nitrogen in the  $\epsilon$ -phase in the region where an oxide film existed earlier leads to the effect of an increase in the depth of the nitride layer during nitriding of a sample that has undergone preliminary oxidation compared to a sample that has undergone nitriding without preliminary oxidation [3].

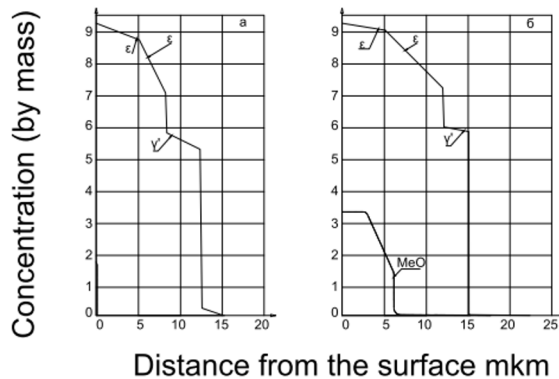


**Fig. 4.** Nitrogen concentration distribution after nitriding without preliminary oxidation (a) and with preliminary oxidation (b). Treatment modes: nitriding: 580°C; 60 minutes; a - preliminary oxidation: 580 °C; 10 min, + Nitriding: 580oC; 60 minutes.

In fig. 4.a shows the calculated distribution curve of the nitrogen concentration in the sample after nitriding without preliminary oxidation, and Fig. 4.b shows the calculated distribution curves of nitrogen and oxygen concentrations in a sample that has undergone preliminary oxidation and subsequent nitriding. This agrees with the experimental results (Fig. 5.). Figure 6. the calculated dependence of the depth of the nitride layer on the time of preliminary oxidation is shown.

However, in Fig. 6, it can be seen that the depth of the nitride layer reaches a maximum as the pre-oxidation time increases, after which it begins to decrease.

This is because with an increase in the oxidation time, the thickness of the oxide film also increases, and while an oxide film exists under the thin nitride layer, the nitride layer practically does not grow [5, 6, 7].

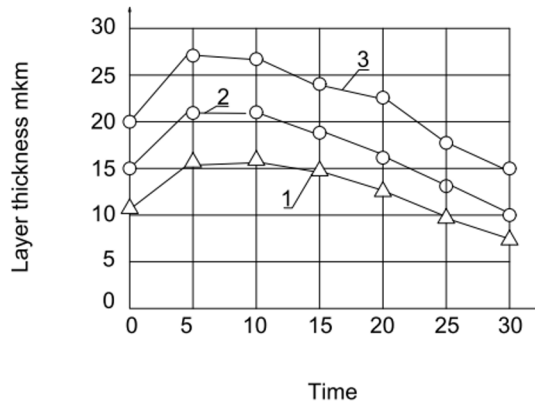


**Fig. 5.** Dependence of nitride layer thickness ( $\mu\text{m}$ ) on pre-oxidation time (min). Temperature  $580^\circ\text{C}$ . Processing modes: preliminary oxidation (10 min.) + nitriding: 1-60 min; 2-120 min; 3-180 min.

Moreover, the nitride layer formed on the surface prevents the release of oxygen into the atmosphere because the oxygen diffusion coefficient near the sample surface decreases.

This circumstance is also considered by the above system of differential equations describing the redistribution process of nitrogen and oxygen concentrations over time. Thus, an increase in the oxidation time decreases the nitriding time since a significant increase in the depth of the nitrided layer begins only when the oxide film completely disappears.

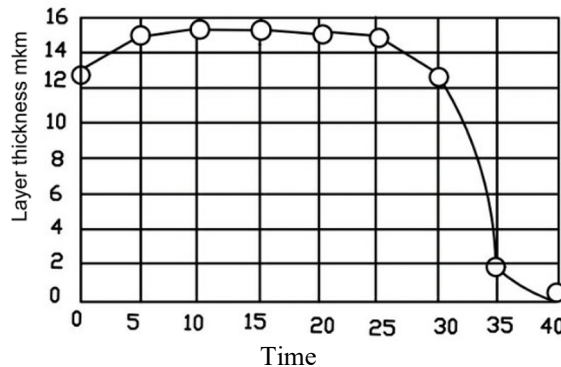


**Fig. 6.** Dependence of thickness of nitrided layer ( $\mu\text{m}$ ) on time of preliminary oxidation (min). Nitriding time - 60 min. Temperature  $580^\circ\text{C}$ .

Thus, during the nitriding of the oxidized sample, two competing processes take place. On the one hand, the presence of oxides of alloying elements in the near-surface layer after the disappearance of the oxide film accelerates the growth of the nitride layer, and the larger the thickness of the oxide film, the larger the region increases the diffusion coefficient of nitrogen in the  $\epsilon$ -phase. On the other hand, the thicker the oxide layer was, the later the nitriding process began [8, 9, 10, 11].

In fig. 7.a shows the distribution of nitrogen concentration after 35 minutes of preliminary oxidation and 60 minutes of nitriding. It can be seen that the depth of the nitride layer is significantly less compared to the regime of 10 minutes of preliminary oxidation and 60 minutes of nitriding (Fig. 4.b). Fig. 7.b it can be seen that after 40 minutes of preliminary oxidation and 60 minutes of nitriding, the nitride layer practically did not begin to grow (because the oxide film, which had grown in 40 minutes of oxidation, did not have time to disappear after 60 minutes of nitriding).

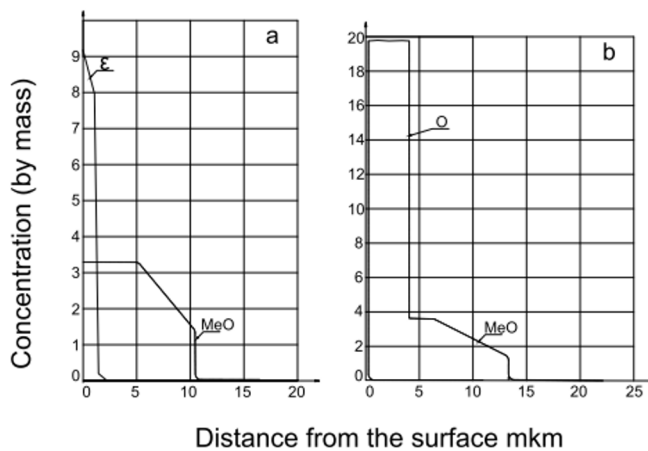


**Fig.7.** Nitrogen concentration distribution after 35 minutes (a) and 40 minutes (b) of preliminary oxidation. Temperature - 580°C. Nitriding time is 60 minutes.

### 3 Results and Discussions

As a result of the studies on contact fatigue and wear resistance, it was found that under conditions of sliding friction with lubrication at low contact loads, wear resistance is increased by a factor of 2.5-3.5 compared to the original nitrided layers. At the same time, the oxide film provides better running-in of the contacting surfaces during friction.

It is shown that the wear resistance of the nitride-oxide coating is 1.5 times higher than the wear resistance of the electroplated chromium coating.

As a result of bench tests of hardened parts, a new nitro-oxidation technology was developed and implemented for the shock absorber rod of a BAAZ car instead of galvanic hard chromium plating.

The new three-stage nitro-oxidation technology has also passed industrial testing at the Rostselmash Production Association for parts operating under wear and atmospheric corrosion conditions.

## 4 Conclusions

1. Thus, analyzing the formation of an oxynitride diffusion protective layer obtained with preliminary and subsequent oxidation, it can be concluded that for each nitriding temperature, there is an optimal preliminary oxidation time, leading to the greatest depth of the nitride layer, leading to the formation of diffusion layers with good physical and mechanical properties.

2. The kinetics of the formation of diffusion nitride-oxide coatings have been studied. It is shown that during short-term preliminary oxidation, the resulting oxide films, consisting mainly of  $\text{Fe}_3\text{O}_4$  with a thickness of 1.0-3.5  $\mu\text{m}$ , provide an acceleration (up to 65%) of the saturation process with nitrogen during nitriding.

3. The microstructure, morphology, and phase composition of nitride-oxide coatings obtained in a three-stage nitro-oxidation regime have been studied.

## References

1. U. R. Boynazarov, T. Kh. Razzokov. Microhardness of diffusion nitroxide layers. Journal "Universum: technical sciences". Russia (2020).
2. U. R. Boynazarov, V. I. Yurshev, L. G. Petrova. Flexural strength of oxynitride coatings. University complex as a regional center of education, science and culture: materials of the All-Russian. Scientific method. conf. (with international participation), pp.490-495, (2020).
3. U. R. Boynazarov, A. A. Karimov. Influence of pre-oxidation on the nitriding process. "Modern materials, technique and technology" Proceedings of the 3rd International Scientific and Practical Conference. Russia (2013).
4. Terent'ev V. F., Michugina M. S., Kolmakov A. G., Kvedaras V., Čiuplys V., Čiuplys A., & Vilys J. The effect of nitriding on fatigue strength of structural alloys. Mechanics, Vol. 64(2), pp.12-22. (2007).
5. Carvalho P., Chappé J. M., Cunha L., Lanceros-Méndez S., Alpuim P., Vaz F., González-Elipe, A. R. Influence of the chemical and electronic structure on the electrical behavior of zirconium oxynitride films. Journal of Applied Physics, 103(10), 104907. (2008).
6. U.R.Boynazarov, T.I.Ergashev. Study of the formation of nitride oxide layers with preliminary oxidation. Universum: Technical Sciences. Vol. 4(85). Russia, Moscow, pp. 87-92. (2021).
7. Boynazarov U. R., Petrova L. G., Brezhnev A. A., and Bibikov P. S. Properties of Oxynitride Steel Coatings Obtained Through Three-Stage Processes of Nitriding Combined with Oxidation. Metallurgist, Vol. 65, pp.886-892. (2021).
8. Liu Z. R., Du J. W., and Chen, L. Influence of oxygen content on structure, thermal stability, oxidation resistance, and corrosion resistance of arc evaporated (Cr, Al) N coatings. Surface and Coatings Technology, Vol. 432, 128057. (2022).
9. Shestopalova L. P. Influence of preliminary oxidation on the subsequent nitriding. Russian Metallurgy, Vol. 2016(13), 1241. (2016).
10. Marônek, M., Bárta, J., Dománková, M., Ulrich, K., & Kolenič, F. (2011). Electron Beam Welding of steel sheets treated by nitrooxidation. Welding in the World, 55(5-6), 10-18.
11. Marônek M., Bárta J., Bártová K., and Dřimal D. Welding of steel sheets treated by nitrooxidation. JOM, 16, 10-13. (2011).